AFRL-RX-TY-TP-2010-0023

COMPUTATIONAL FLAME CHARACTERIZATION OF NEW LARGE AIRCRAFT IMMERSED IN ACCIDENTAL HYDROCARBON POOL FIRES

Christopher P. Menchini
Applied Research Associates
4300 San Mateo Blvd, N.E.
Albuquerque, NM 87110

John Hawk
Air Force Research Laboratory, Airbase Technologies Division
139 Barnes Drive, Suite 2
Tyndall Air Force Base, FL 32403-5323

Contract No. FA4819-09-C-0030

MARCH 2010

AIR FORCE RESEARCH LABORATORY
MATERIALS AND MANUFACTURING DIRECTORATE

■ **Air Force Materiel Command** ■ **United States Air Force** ■ **Tyndall Air Force Base, FL 32403-5323**

REPORT DOCUMENTATION PAGE

Form Approved
OMB No. 0704-0188

1. REPORT DATE *(DD-MM-YYYY)*	2. REPORT TYPE	3. DATES COVERED *(From - To)*
31-MAR-2010	Presentation PREPRINT	14-FEB-2010 -- 03-MAR-2010

4. TITLE AND SUBTITLE
Computational Flame Characterization of New Large Aircraft Immersed in Accidental Hydrocarbon Pool Fires (BRIEFING SLIDES)

5a. CONTRACT NUMBER
FA4819-09-C-0030

5b. GRANT NUMBER
N/A

5c. PROGRAM ELEMENT NUMBER
99999F

6. AUTHOR(S)
Menchini, Christopher P.; Hawk, John

5d. PROJECT NUMBER
GOVT

5e. TASK NUMBER
D0

5f. WORK UNIT NUMBER
Q130D6AG

7. PERFORMING ORGANIZATION NAME(S) AND ADDRESS(ES)
Applied Research Associates
4300 San Mateo Blvd, N.E.
Albuquerque, NM 87110

8. PERFORMING ORGANIZATION REPORT NUMBER

9. SPONSORING/MONITORING AGENCY NAME(S) AND ADDRESS(ES)
Air Force Research Laboratory
Materials and Manufacturing Directorate
Airbase Technologies Division
139 Barnes Drive, Suite 2
Tyndall Air Force Base, FL 32403-5323

10. SPONSOR/MONITOR'S ACRONYM(S)
AFRL/RXQD

11. SPONSOR/MONITOR'S REPORT NUMBER(S)
AFRL-RX-TY-TP-2010-0023

12. DISTRIBUTION/AVAILABILITY STATEMENT

Distribution Statement A: Approved for public release; distribution unlimited.

13. SUPPLEMENTARY NOTES
Ref AFRL/RXQ Public Affairs Case # 10-0xx. Document contains color images. For presentation at the 2010 FAA Worldwide Airport Technology Transfer Conference, 20-22 April 2010, Atlantic City, NJ.

14. ABSTRACT

This briefing describes the AFRL program for aircraft crash-rescue and fire fighting operational support and proposes test concepts for the evaluation of fire fighting agents and technology.

15. SUBJECT TERMS

fire, new large aircraft computational fluid dynamics, ARFF, aircraft mishap

16. SECURITY CLASSIFICATION OF: a. REPORT	b. ABSTRACT	c. THIS PAGE	17. LIMITATION OF ABSTRACT	18. NUMBER OF PAGES	19a. NAME OF RESPONSIBLE PERSON
U	U	U	UU	26	R. Craig Mellerski, DR-III

19b. TELEPHONE NUMBER *(Include area code)*
850-283-3744

Reset

Standard Form 298 (Rev. 8/98)
Prescribed by ANSI Std. Z39.18

COMPUTATIONAL FLAME CHARACTERIZATION OF NEW LARGE AIRCRAFT IMMERSED IN ACCIDENTAL HYDROCARBON POOL FIRES

20 April 2010

JOHN R. HAWK, P.E.
Senior Engineering Advisor
Materials & Manufacturing Directorate
Air Force Research Laboratory

CHRISTOPHER P. MENCHINI
Senior Engineer (Contractor)
Applied Research Associates, Inc.

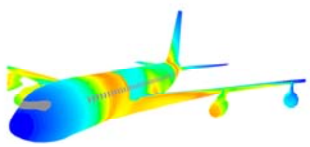

Introduction

- **Goal**
  - Develop an efficient computational strategy to predict the flame characteristics and thermal response of aircraft structures immersed in hydrocarbon pool fires
  - Apply strategy to crash fire scenarios of interest to the FAA and AFRL (e.g. past accidental fire case studies, novel commercial / military aircraft platforms)
  - Integrate into an aircraft-crash-fire simulation framework

- **Motivation**
  - Full-scale aircraft hydrocarbon pool fire testing is expensive and arduous
  - The FAA is concerned with unique fire protection challenges New Large Aircraft (NLA) pose due to unusually great dimensions, fuel quantities, and novel (composite) materials

2

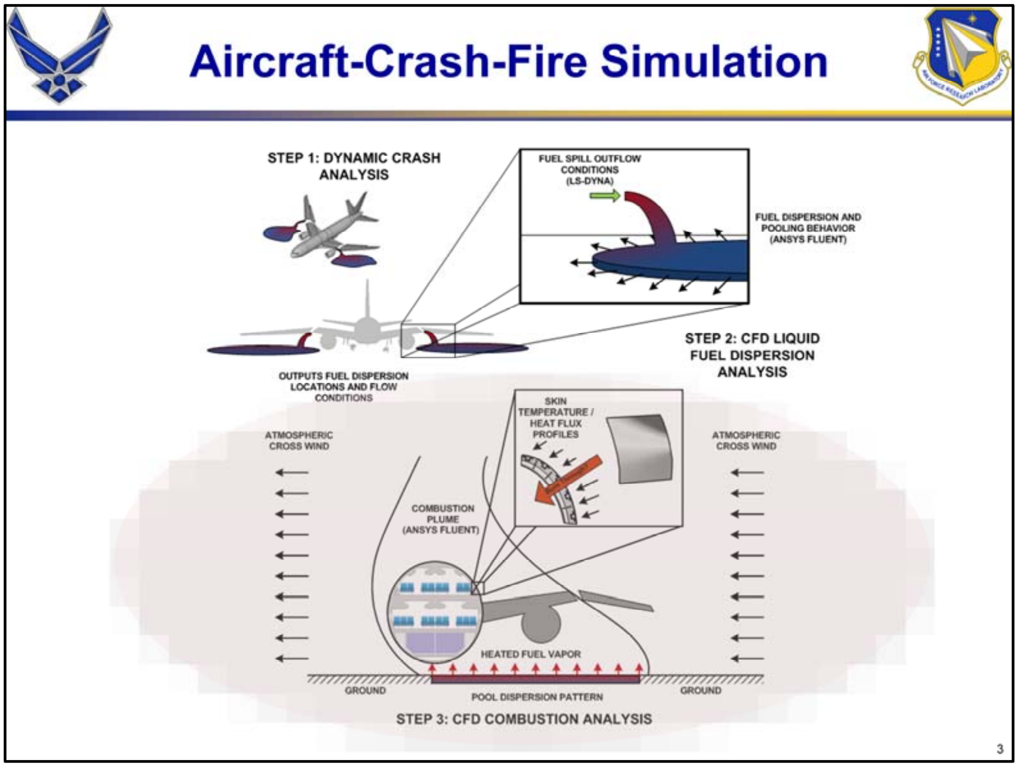

A multi-tiered simulation framework is being formulated to model a sequential dynamic aircraft crash fire event. Applied Research Associates SVO is developing a phase I aircraft crash analysis methodology, with the AFRL/RXQD following suit working on a phase II liquid fuel dispersion and phase III combustion analysis using computational fluid dynamics.

Technical Challenges

- **Computational efficiency**
  - Accuracy vs. Predictability
- **Experimental validation data**
  - Confidence Levels / Repeatability / Expense
- **Multiple non-linear PDEs governing complex flow physics**
  - Combustion / Heat Transfer / Turbulence / Multiphase Flow
- **Wide range of spatial and temporal scales**
  - Airbus A380 ϑ(100's m) vs. Turbulent dissipative length scales ϑ(mm)

HARDWARE RESOURCES

MULTI-SCALE
TURBULENT FIRE PLUME

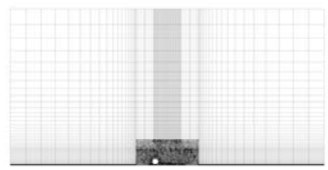

MESH TOPOLOGY
OPTIMIZATION

4

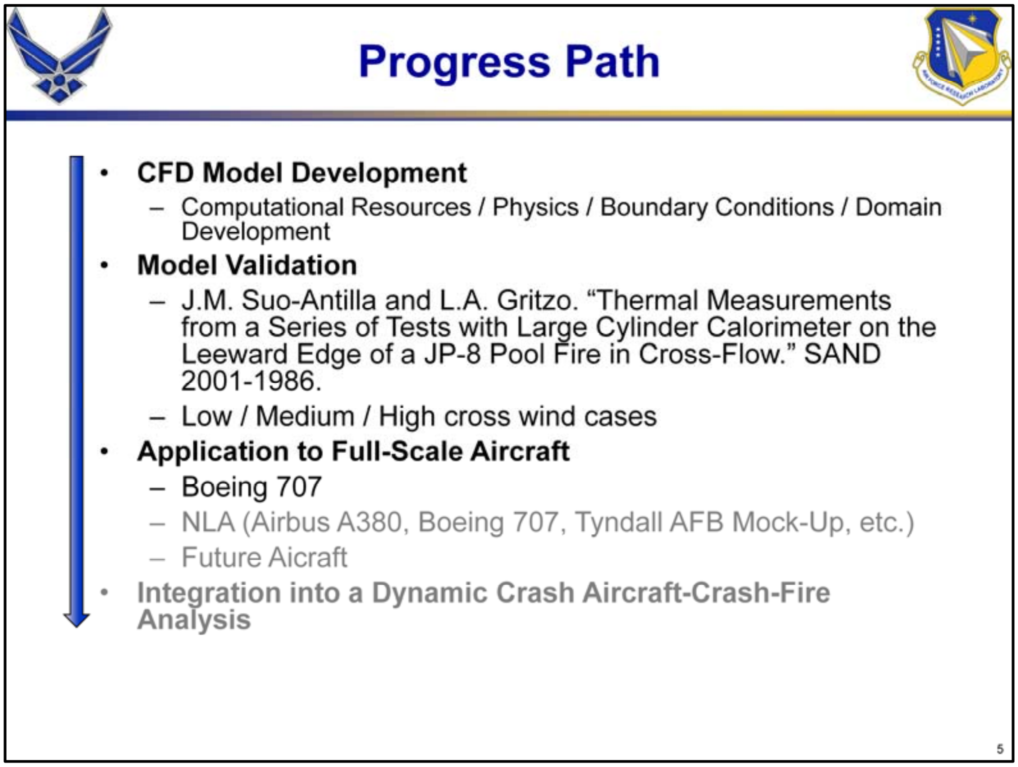

The bullets are faded at the bottom of slide 5 because it's a progress path and those items have not been completed yet.

CFD Model Development: Physics

- **ANSYS Fluent 12.1: 11 Equation Model**
  - 3-D Navier-Stokes (5)
  - Non-Premixed Combustion (Mixture Fraction PDF) Approach (2)
  - Realizable k-ε (RANS) Turbulence (2)
  - Discrete Ordinates (DO) (1)
  - Single Step Khan and Greeves Soot Model (1)

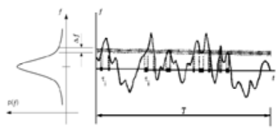

PROBABILITY DENSITY FUNCTION (PDF)

ANSYS Fluent Theory Guide (2009)

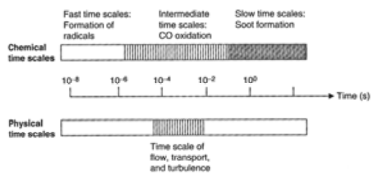

TURBULENT - CHEMISTRY INTERACTION

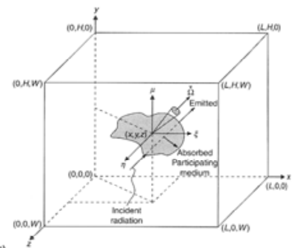

DO RADIATION DISCRETIZATION

"CFD in Fire Engineering." Yeoh and Yuen (2009)

6

CFD Model Validation: Experiment

- **Low / Med / High Cross Winds Over a Cylinder**

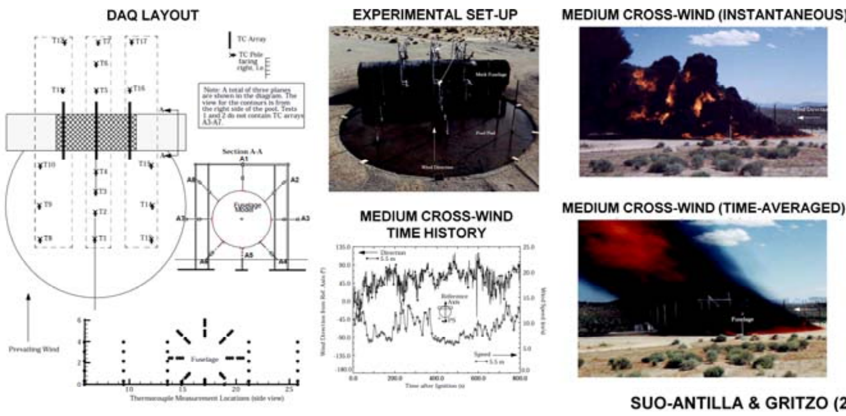

SUO-ANTILLA & GRITZO (2001)

Case Name	Time After Ignition (s)	Wind Velocity ($m \cdot s^{-1}$)	Wind Direction (°)
Low	225 – 350	1.9 ± 0.2	-36.9 ± 5.7°
Medium	400 – 575	5.4 ± 1.2	-11.4 ± 12.5°
High	300 – 600	10.2 ± 1.7	-22.7 ± 8.3°

7

Sandia National labs has developed an experimental test series designed specifically to provide flame and skin temperature and heat flux data on a cylinder immersed in a jet fuel fire under varied wind conditions. Certain segments of their data was extracted and averaged due to optimal quasi-steady wind conditions. A low, medium, and high wind data set was selected from their data reduction to formulate a comparable modeling environment to compare results.

CFD Model Validation: Model Set-Up

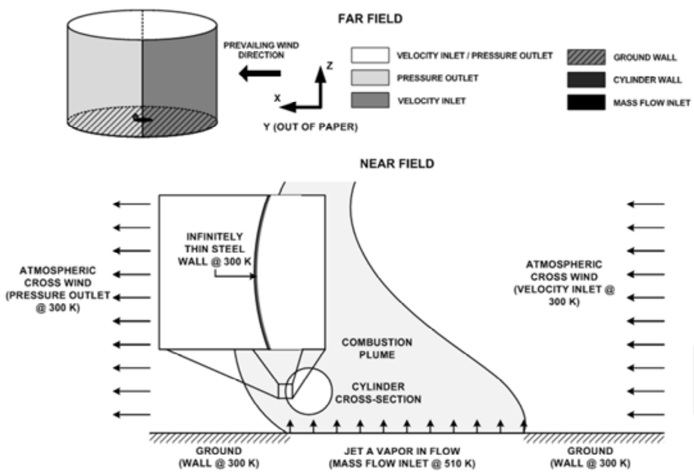

Fire Inlet Condition	Value
Flow Rate ($kg \cdot m^{-2}s^{-1}$)	0.058
Temperature (K)	510

Case Name	Mean Wind Velocity (ms^{-1})	TI (%)	Reynolds Number (Re_{cyl})
Low	1.9	10.5	4.76×10^5
Medium	5.4	22.2	1.35×10^6
High	10.2	16.7	2.56×10^6

Note: The characteristic turbulent length scale used for all cases is 0.256 m

8

The following boundary conditions were set reflecting measurements and observations made by Sandia National labs to create similar physical conditions. Far field model boundaries were defined to simplify model orientation with respect to the oncoming measured wind direction from experiments. The fire inlet conditions were extrapolated from Sandia experimental data and turbulent boundaries conditioned to reflect the fluctuations measured.

All wall conditions were initialized to 300 K, but were allowed to float (or rise) during the CFD solution process to account for combustion convective and radiant heat transfer effects.

Reynolds number calculations are based upon the cylinder diameter, and reflect an increasing turbulent flow regime due to increasing mean velocity validating the need for turbulent versus laminar flow modeling assumptions.

CFD Model Development: Domain

- **Pointwise Gridgen 15: Multi-Block Hybrid Topology**
  - Structured (hexahedral) high aspect ratio cells used for far field atmospheric boundary layer development and cylinder boundary layer growth
  - Unstructured (tetrahedral) cells used to link structured blocks

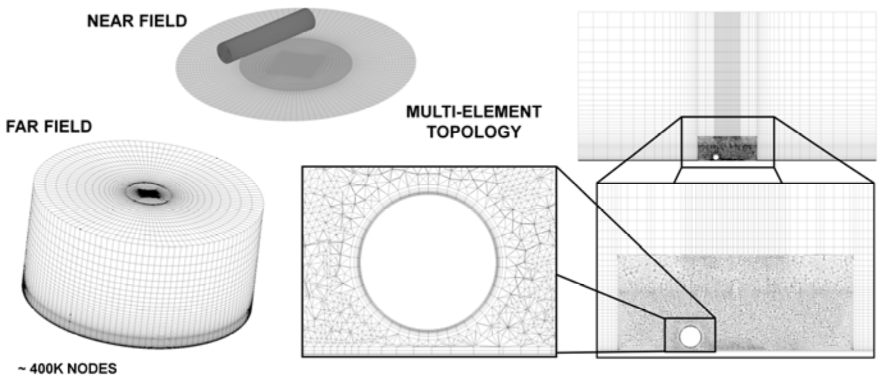

9

CFD Model Validation: Model Set-Up

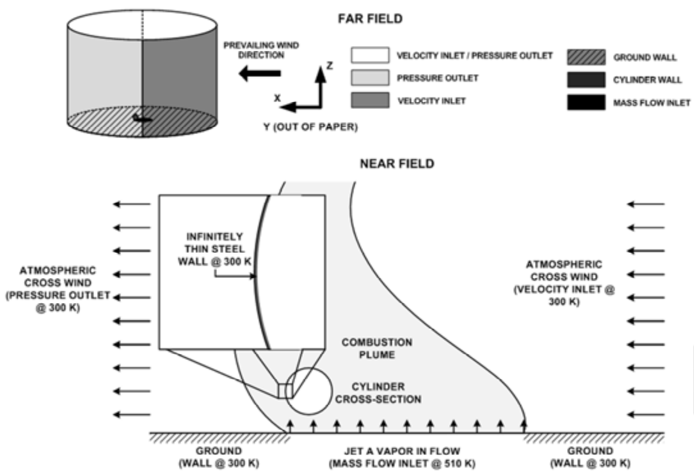

Fire Inlet Condition	Value
Flow Rate (kg·m^{-2}s^{-1})	0.058
Temperature (K)	510

Case Name	Mean Wind Velocity (ms^{-1})	TI (%)	Reynolds Number (Re_{cyl})
Low	1.9	10.5	4.76×10^5
Medium	5.4	22.2	1.35×10^6
High	10.2	16.7	2.56×10^6

Note: The characteristic turbulent length scale used for all cases is 0.256 m

10

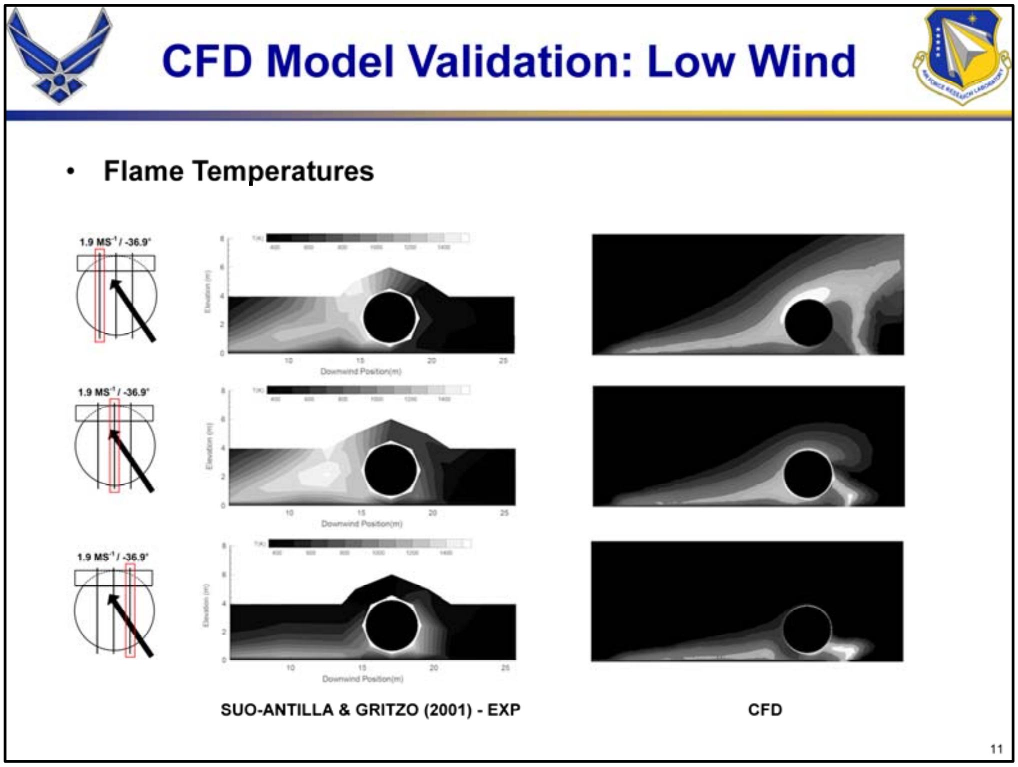

Low wind flame temperature measurements compare very well with model results, especially when taking into account dissimilarities between experimental set-up and model conditions.

The low cross-wind conditions create the best conditions for a pure diffusion flame compared to the higher wind conditions, reflecting an environment most representative of the model design assumptions.

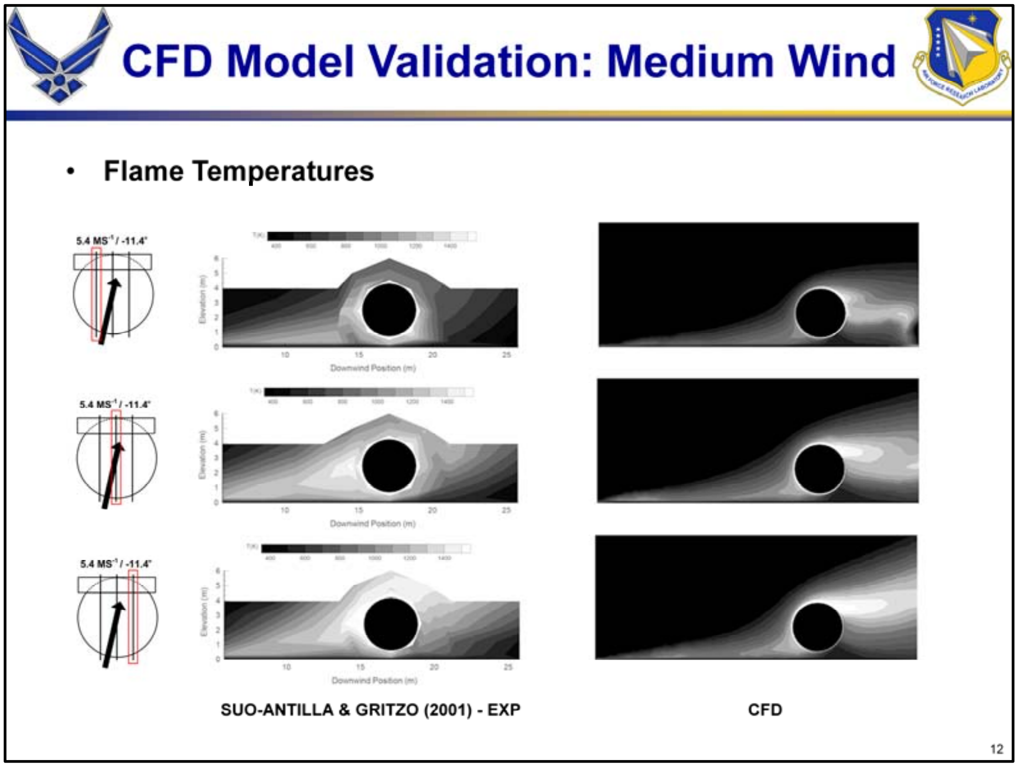

The medium wind comparative condition compares reasonably well like the low wind condition, with the most normally distributed wind gust across the cylinder. With the highest turbulence intensity measured of all three cases, this case provides the most even and well-averaged results most favorable for turbulent RANS modeling conditions.

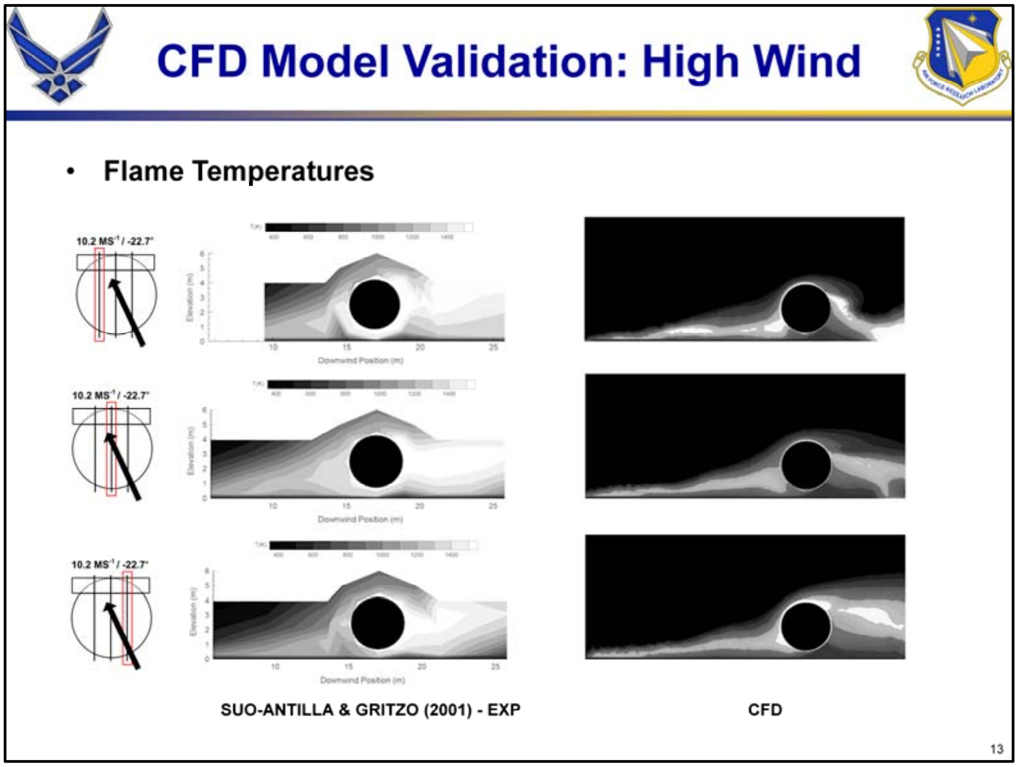

The high wind validation case shows the highest discrepancy of all three cases for 2 primary reasons. Here, the convective force of the cross wind condition begins to compete heavily with the diffusion combustion process creating a fire plume nearing the modeling assumption limitations. In addition, increased cross winds create greater flow separation around the leeward side of the cylinder. With the employment of a reduced order (2-equation linear eddy-viscosity) turbulence model to save computational cost, cylinder flow separation and ultimate detachment becomes increasingly hard to predict, shifting average flamelet location off of the cylinder surface. This creates large discrepancies between skin temperatures and heat fluxes leading to the largest divergence between experimental and model results.

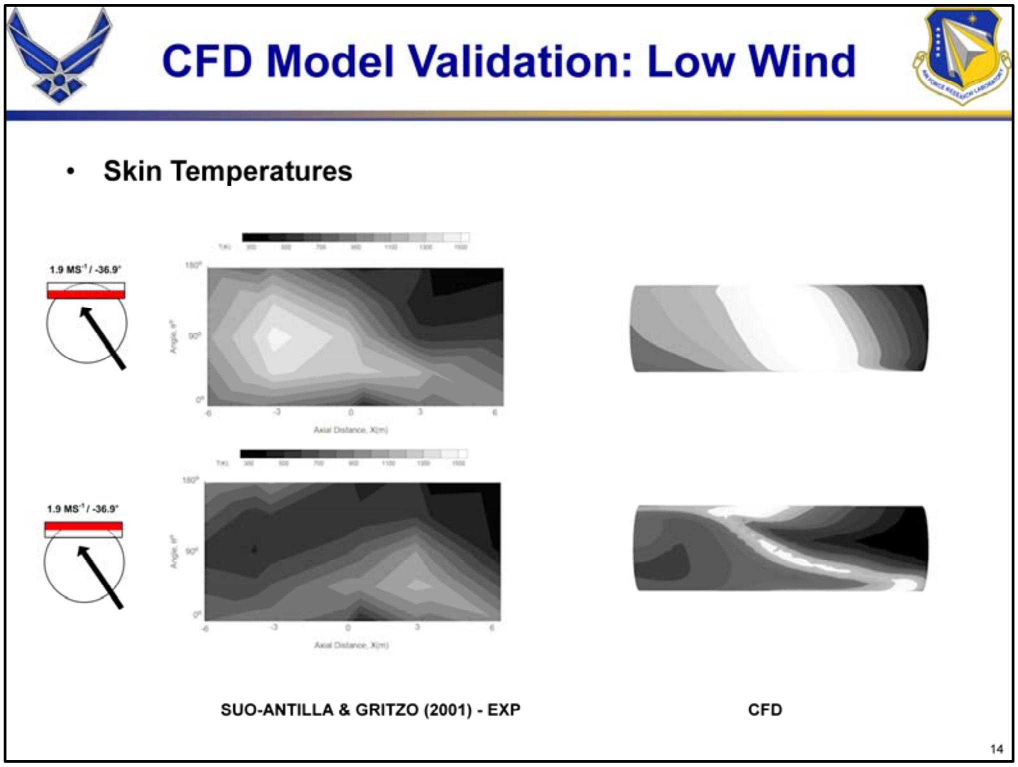

Low speed skin temperature modeling results reflect reasonably well compared to experiment once again when taking into account all of the model simplifications. Maximum temperature magnitudes are achieved and trends are generally comparable.

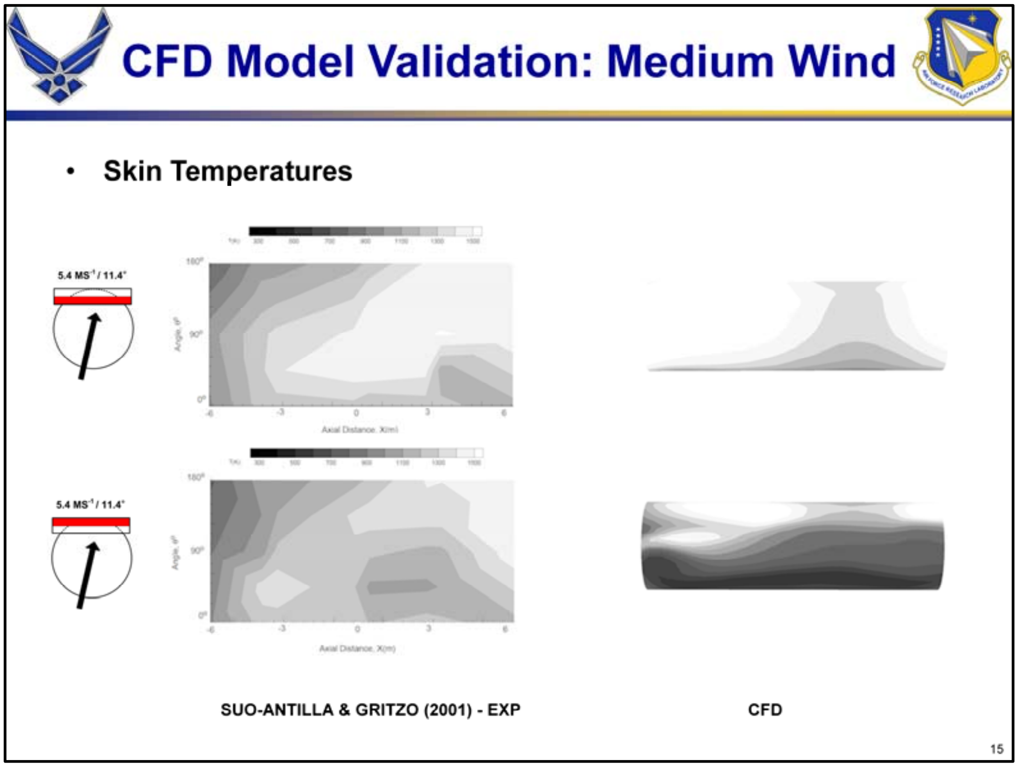

Similar to the low wind case, medium wind conditions create favorable results as well with applied conditions still well within model assumptions.

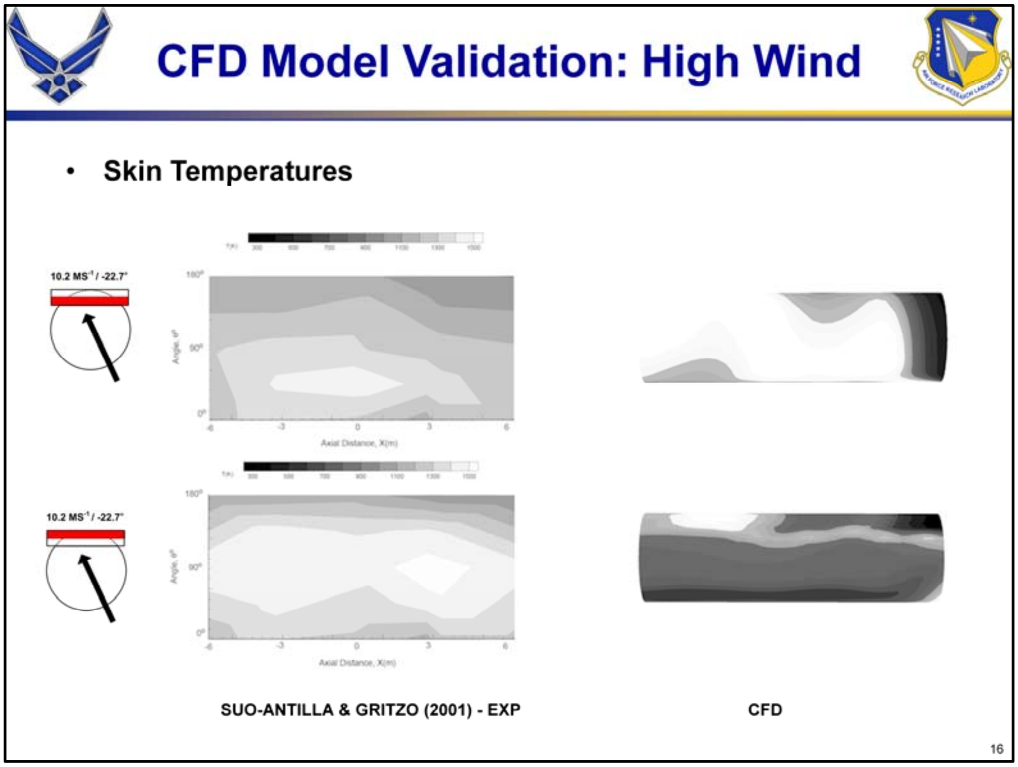

Model issues with flow separation become largely apparent here with windward surface temperatures comparing reasonably well with experimental results, but the leeward cylinder side diverging significantly due to the flame lifting off of the surface.

Flame lifting can be caused by a combination of both turbulent flow model breakdown combined with combustion model assumption divergence.

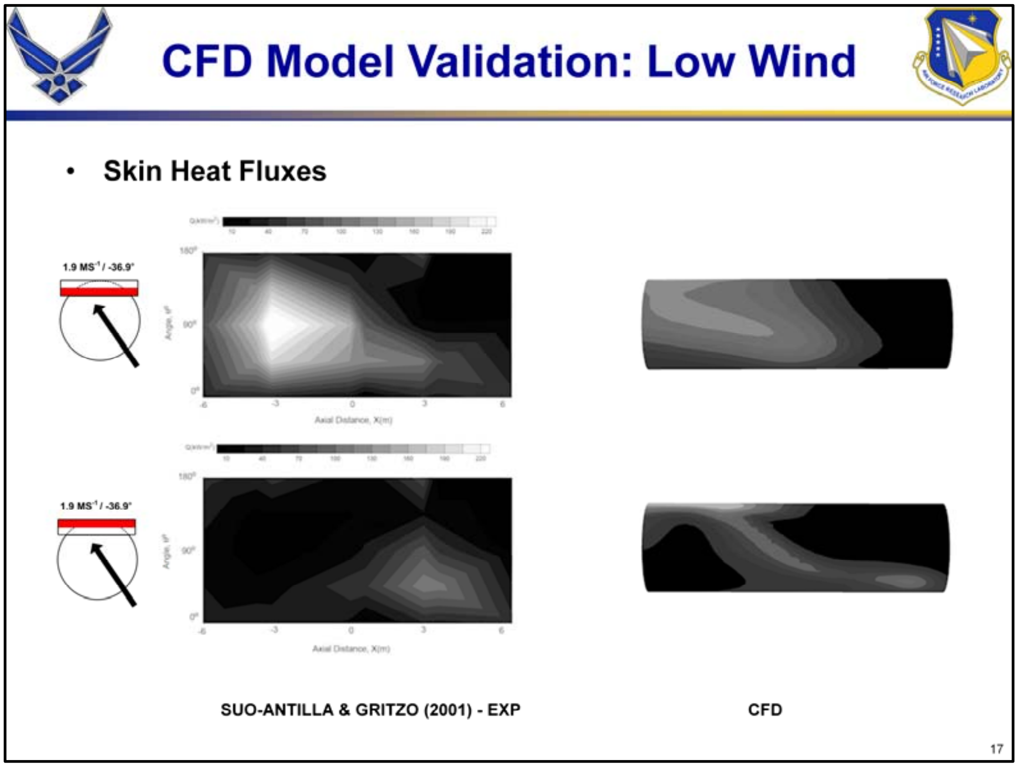

Heat flux magnitudes tend to follow suit with skin temperature measurements, with the low wind condition creating acceptable heat flux magnitudes and trending profiles between model and experiment.

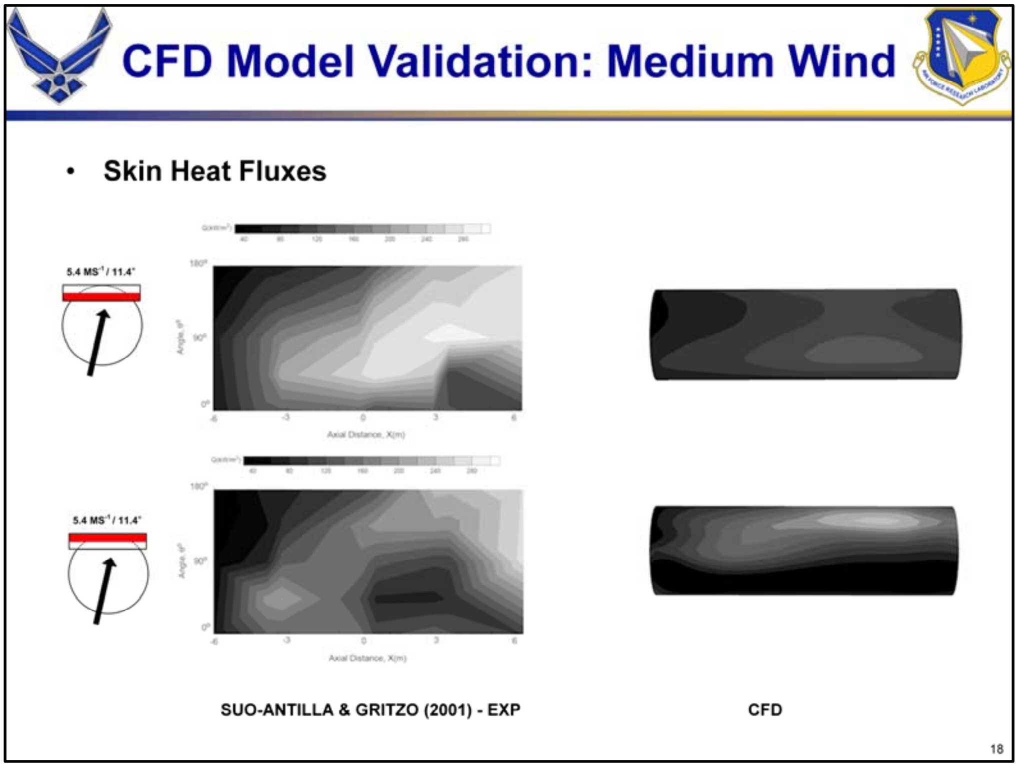

Although heat flux model and experimental magnitudes aren't as comparable compared to the low wind speed case, the profiles compare well showing major flow structures are well captured.

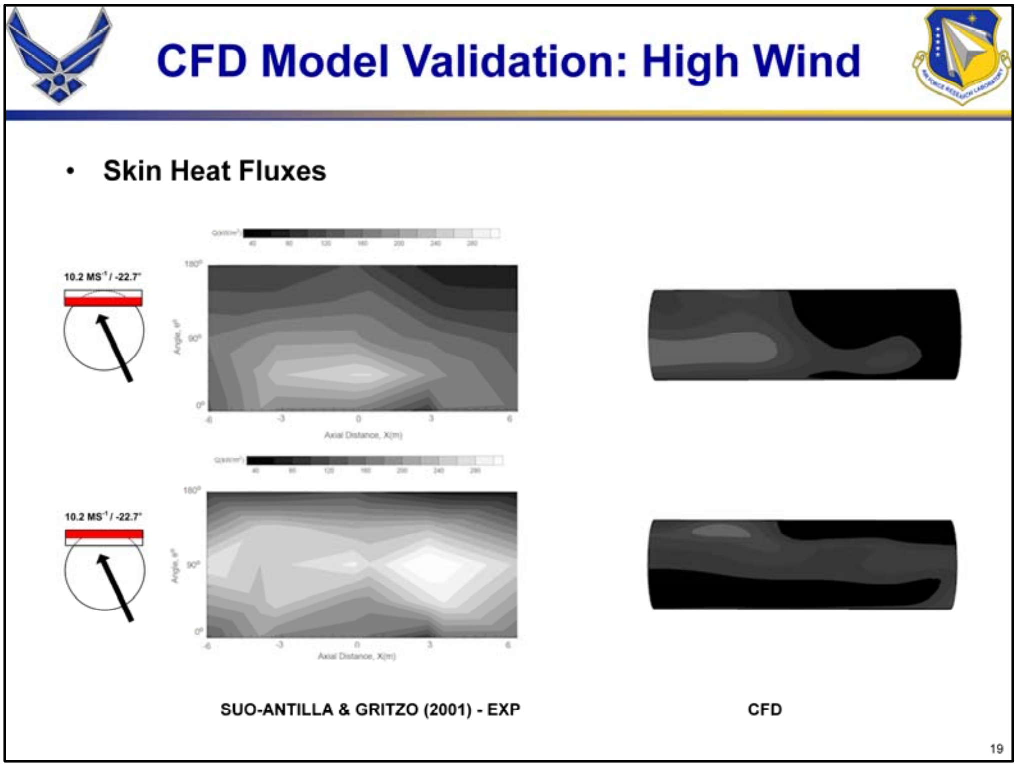

Leeward heat flux comparisons between model and experiment suffer the most for the high wind regime for the same reasons discussed previously. Heat flux magnitudes and trending profiles, however, due compare well on the windward side where flow separation is not an issue.

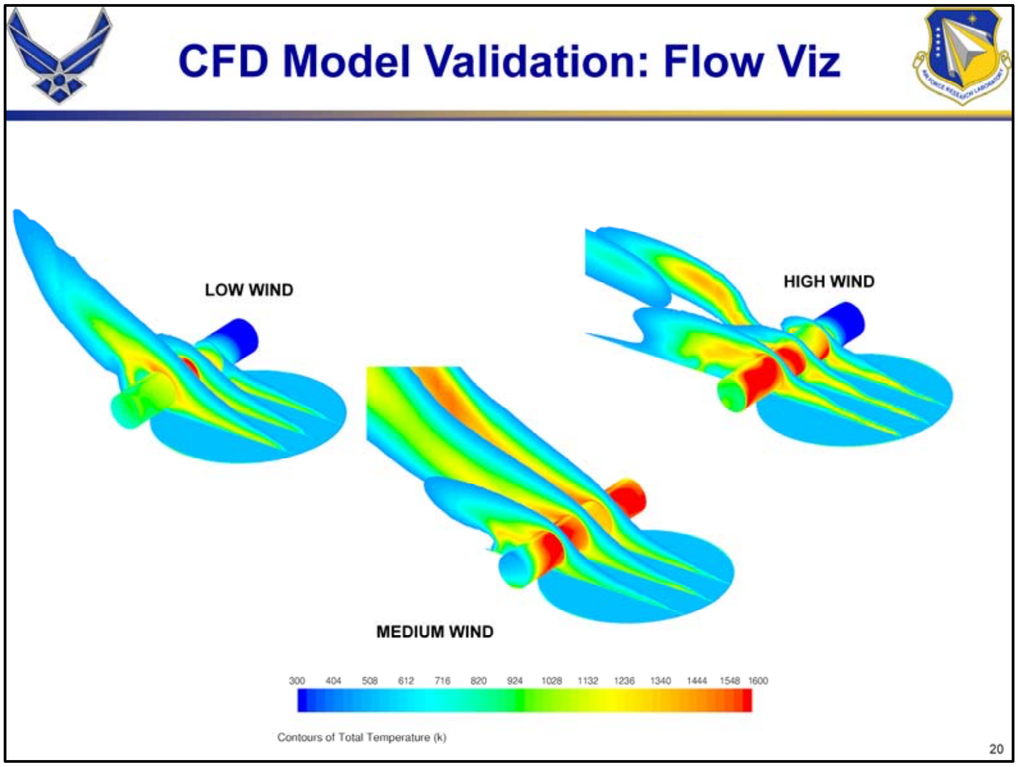

The following three pictures depict the average flame shape and temperature in the 3 cross-cuts compared against experimental data, in addition to cylinder skin temperatures.

The low wind case shows the lowest plume temperatures largely due to the least amount of fuel air mixing combined with the largest off normal wind direction with respect to the cylinder surface.

The medium wind case has the highest fluctuating wind condition and the most normal wind direction creating the most definitive plume shape and increased temperatures.

The high wind case had the least amount of wind fluctuations but the highest magnitudes causing increased swirl behind the cylinder and non-coherent plume structures.

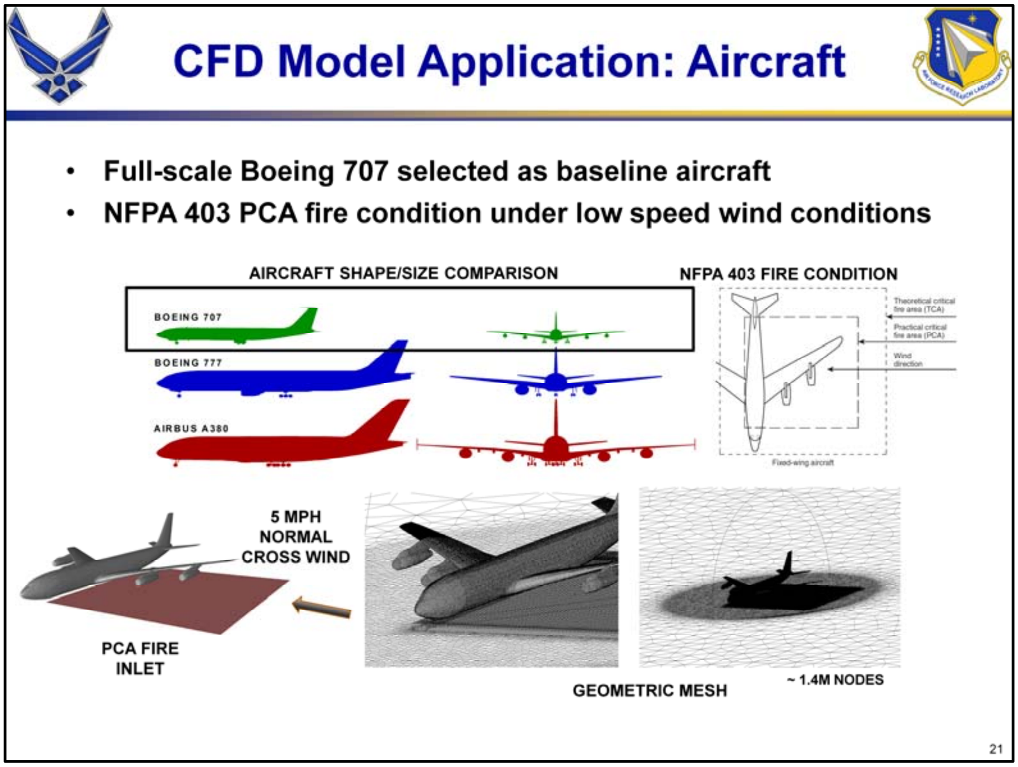

The Boeing 707 was selected as the baseline aircraft due to its comparable size and shape with the average commercial jetliner.

The PCA fire condition as described in NFPA 403 was used for model conditions, with formal boundary conditions derived from the low to medium cross-wind speeds that compared the best in the validation study.

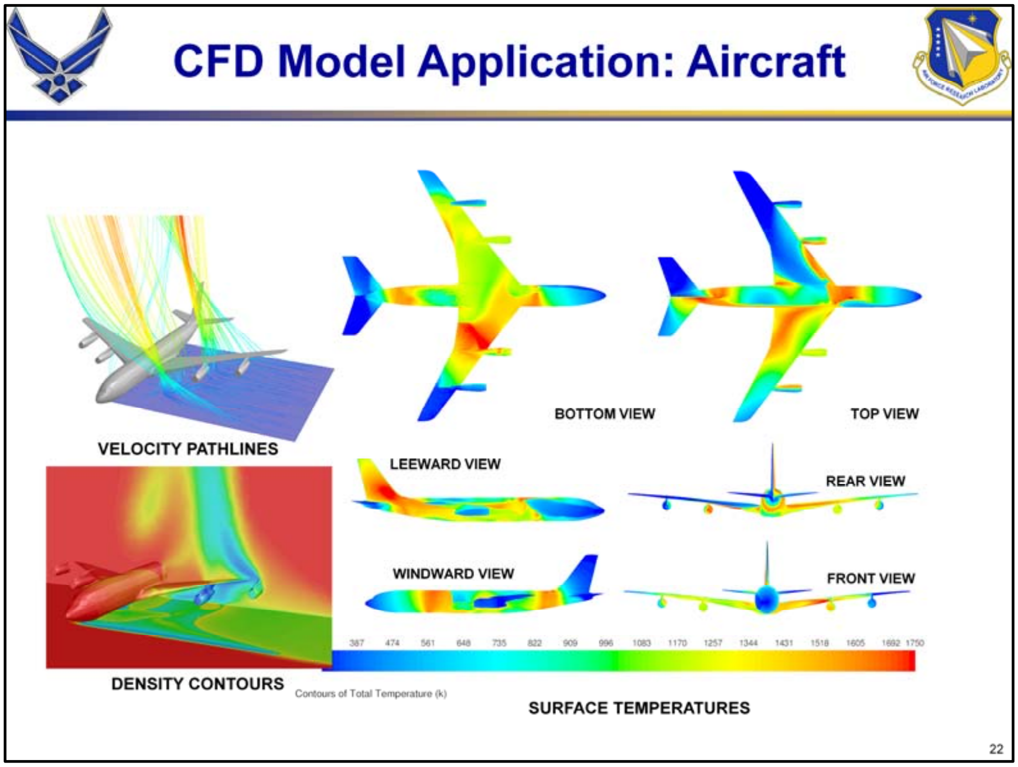

Flow visualization of the Boeing 707 in a 5 mph (equivalent low speed condition) with 10% turbulence intensity is depicted.

Similar to the validation cylinder results, thermal surface conditions are affected by the local flow structures created by the turbulent mixing between the combusting fuel vapors and incoming oxygenated wind. More complex surface shapes create a more varied profile creating localized hot and cold spots due to varied aerodynamic shapes (stream-wise main wings versus the bluff body the vertical tail presents to the oncoming cross-flow).

Conclusions

- Experimental flame and skin temperatures compare well profile trend and magnitude-wise to CFD at low to medium wind velocities, with the largest discrepancies in the high wind regime
- Cylinder flow separation appears to be a first order turbulent flow modeling effect leading to the divergence on the leeward cylinder surface thermal effects
- Sharp flamelet gradients are indicative of fast chemical kinetic time scales largely absent in the "mixed-is-burnt" model based upon slower fluid motion time scales
- Simple soot modeling provides sufficient radiant heat absorption to accurately meter total heat transfer magnitudes, but lacks in qualitative plume size and shape prediction
- Full-scale aircraft thermal and fluid structures trend similarly to the validation study, with resource needs increasing by about 4x.

Future Work

- Analyze alternative CFD sub-models (combustion / turbulence / soot) to increase accuracy
- Gather more validation / material property data
- Run unsteady cases to determine transient effects and examine material heat up times
- Complete Airbus A380 and Boeing 787 case studies (Possibly Tyndall AFB Airbus Mock-Up?)
- Apply to alternate aircraft / combustion scenarios of interest
- Ultimate integration into an aircraft-crash-fire simulation framework.

24